ANL/NSE-18/12

User Manual for MC²-3 Gamma Library Generation

Revision 0

Nuclear Science and Engineering Division

ANL/NSE-18/12

User Manual for MC^2-3 Gamma Library Generation

Revision 0

prepared by

Changho Lee
Nuclear and Science Engineering Division, Argonne National Laboratory

Byoung Kyu Jeon and Won Sik Yang
Nuclear Engineering & Radiological Sciences, University of Michigan

October 10, 2018

ABSTRACT

This document presents a detailed description of generating the gamma library for MC^2-3 which includes delayed gammas and betas based on the 94 gamma energy groups. The updated methodologies associated with heating and gamma calculations are introduced, which account for the self-shielding effect on KERMA factors and perform the gamma transport calculations to condense the gamma data from 94 to 21 groups. For these updates, the PreGAMMA code was developed to prepare NJOY inputs and generate delayed gammas and betas, and the GenGAMMA code was updated to process the outputs of PreGAMMA and NJOY. This document briefly discusses verification results of the new gamma library using the ABTR fuel pin and the EBR-II benchmark problem.

REVISION HISTORY

Revision	Description
0	Initial release: October 10, 2018 Associated PreGAMMA and GenGAMMA versions: 1.0.0 Associated MC^2-3 version: 3.2.3

TABLE OF CONTENTS

LIST OF FIGURES

LIST OF TABLES

1. Introduction

In fast reactor design analyses, a coupled neutron and gamma heating calculation needs to be carried out to accurately evaluate the heat source distribution in the core. The coupled neutron and gamma heating calculation requires gamma production and interaction cross sections and KERMA (Kinetic Energy Release in Materials) factors as well as neutron interaction cross sections. The MC^2-3 code [1] has a complete capability of generating neutron cross sections (ISOTXS), gamma production and KERMA factors (PMATRX) and gamma interaction cross sections (GAMISO) for use in core calculation codes like DIF3D. For gamma calculations, the current 21 group gamma library generated from the NJOY code [3] has been used and verified against the EBR-II benchmark problem [2]. However, the gamma library has some deficiencies in terms of a self-shielding of KERMA factors, delayed gammas and betas, and the number of gamma groups.

In order to improve the gamma production accuracy, a new gamma library was developed which includes delayed gammas based on the 94 gamma energy groups and delayed betas. In addition, the methodologies associated with heating and gamma calculations were improved by accounting for the self-shielding effect on KERMA factors and performing the gamma transport calculations for condensing the gamma data from 94 to 21 groups. For these updates, the PreGAMMA code was developed to prepare NJOY inputs and generate delayed gammas and betas, and the GenGAMMA code was updated to be able to process the outputs of PreGAMMA and NJOY.

This document describes the procedure of generating the gamma libraries of MC^2-3 along with the updated methodologies and some verification results. In Section 2, the new procedure and computational methods for gamma library generation are presented, including PreGAMMA (a preprocessing code for gamma library generation) and GenGAMMA (a code for generating the MC^2-3 gamma library). The new gamma transport capabilities of MC^2-3 associated with the new gamma libraries are discussed in Section 3. Section 4 briefly introduces verification results of the updated libraries and gamma transport capabilities of MC^2-3 for the ABTR fuel pin cell problem [6]. A summary is provided in Section 5.

2. New Procedure for Generation of Gamma Libraries of MC^2-3

2.1 New Gamma Library Processing Code

A procedure of generating the gamma libraries of MC^2-3 was established by developing pre- and post-processing tools for the NJOY code. The procedure eliminates a cumbersome user input preparation for individual isotopes required for running NJOY and thus potential input errors. Figure 1 schematically shows the code system and procedure used in generating the new gamma libraries. The PreGAMMA was developed to prepare the NJOY input files and generate delayed gamma libraries, and several modifications were made in the GenGAMMA code processing the NJOY output. The PreGAMMA code is able to prepare NJOY input files for generation of multigroup gamma interaction cross sections and heating factors as well as for generation of multigroup neutron cross sections, neutron heating factors and gamma production matrices. PreGAMMA also prepares a batch file to execute NJOY and an input file for GenGAMMA. The PreGAMMA and GenGAMMA code are programmed in standard Fortran 90+ and compatible with Windows and Linux OS environments.

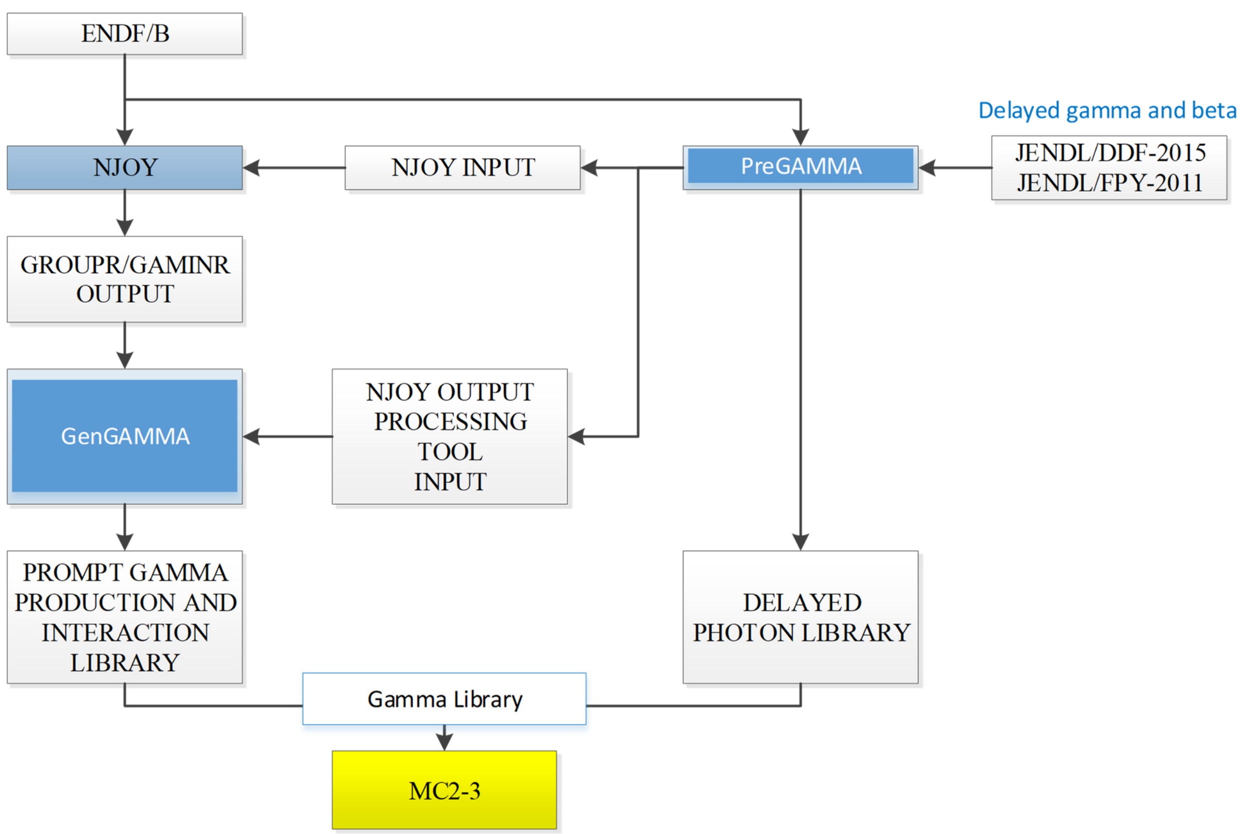

Figure 2-1. Calculation Flow for Gamma Libraries of MC^2-3

The PreGAMMA code is composed of five main functions: input processor, generation of input files for NJOY and GenGAMMA, generation of a batch file to run the NJOY code, processing of decay and fission yield libraries, generation of delayed gamma libraries. PreGAMMA requires the paths of two code executables (NJOY99.396 and GenGAMMA) and the directories of five base libraries (neutron interaction, thermal scattering, photo-atomic reaction, decay data, and fission yield libraries). The PreGAMMA code produces principle neutron cross sections and scattering matrices for the isotopes specified in an input file. PreGAMMA performs additional action to generate gamma or thermal sublibraries of MC^2-3 when the sublibrary options are specified in the input file. The detailed descriptions of an input file and output files of the PreGAMMA code are given in the input description section.

The GenGAMMA code was originally designed to generate principle cross sections and scattering matrices by processing a GENDF tape (groupwise-ENDF file), produced by the GROUPR module of NJOY. The GenGAMMA code has recently been updated to translate the GENDF file into the gamma libraries of MC^2-3 since the GENDF file contains gamma interaction cross section vectors, neutron-induced photon production matrices, neutron and gamma heating and damage factors as well as the neutron cross sections. The GenGAMMA code reads the corresponding data and converts them into an appropriate form to be used in MC^2-3. The detailed procedure is summarized for each group constant type in each subsection, and the format of new gamma library of MC^2-3 is given in the later section.

The new gamma libraries of MC^2-3 were generated using 2,082 neutron and 94 gamma group structures. The group structures were selected based on the MC^2-3 neutron ultrafine group structure and the 94-gamma group structure of the Cross Section Evaluation Working Group (CSEWG) [3]. The 94-group structure covers the energy range from 5 keV to 20 MeV, and it is considered to represent the smooth gamma interaction cross section properly for the energy range of interest in the gamma heating calculation. In the latest ENDF/B-VII.1 files, the neutron interaction cross sections are evaluated for 423 isotopes and the photo-atomic sublibrary is given for 100 materials. It is noted that the PreGAMMA code automatically bypasses the Cl-35 isotope in the process, since the Reich-Moore Limited resonance representation used for Cl-35 cannot be processed by the NJOY99 code. The PreGAMMA will be updated in the near future to facilitate the NJOY2012 code, which is capable to process the Reich-Moore Limited format.

2.2 Prompt Gamma Production Yield Matrix

The photon production cross section refers to the probability that a neutron in a neutron group would produce a certain number of photons in a photon group. In the ENDF, the photon production cross section is computed by combining the cross sections from File 2 and/or File 3 and the corresponding photon production multiplicities in File 12 or is directly obtained from the prompt photon production cross section data in File 13. File 12 generally contains the major photon production data with the appropriate MT numbers, including low-level discrete inelastic scattering. File 13 is used to gather the rest of photon production data from all remaining reactions, which cannot be separable at high energy. File 15 contains the energy distributions of emitted photons. In ENDF-6 format, photon production subsections also appear in File 6. Thus, the GROUPR module of NJOY generates neutron-photon matrix by combining the data in Files 2, 3, 6, 12, 13 and 15. The PreGAMMA code first checks the availabilities of these file numbers for each isotope, and then prepares the input files for the NJOY runs in such a way that those files are properly coordinated in the production matrix generation. Note that the PreGAMMA code utilizes the data in File 6 only when the photon cross sections for non-elastic reaction are not given in File 13, MT 3.

The photon production cross sections generated in the 2,082 neutron group structure through the NJOY calculations are not self-shielded because the cross sections are condensed at the infinite dilute condition. The use of unshielded photon production cross sections in the gamma source calculation would yield over-estimated gamma production rates for capture and fission reactions. Moreover, these production rates are inconsistent with the actual reaction rates obtained from a neutron transport calculation because the self-shielded capture and fission cross sections prepared by MC^2-3 are used in the neutron transport calculation. In order to circumvent this inconsistency problem, the gamma production cross sections for capture and fission reactions are converted into yield matrix by dividing the production cross section by the neutron cross section. Later, the self-shielded production cross sections for capture and fission reactions are calculated in MC^2-3 by multiplying the yield matrices with self-shielded cross sections. For non-elastic neutron reactions, the production matrices are directly provided in the gamma library and utilized without the intermediate process.

2.3 Neutron KERMA Factors

A KERMA factor is defined as an averaged kinetic energy release per reaction times a cross section [3]:

$$k_{ij}(E) = \sum_{l} \overline{E}_{ijl}(E)\sigma_{ij}(E), \tag{1}$$

where $\overline{E_{ijl}}$ is the total kinetic energy carried away by the l^{th} species of secondary particles, and σ_{ij} is the cross section for material i and reaction j. The neutron KERMA factors are calculated in the HEATR module of NJOY as a pointwise cross section. However, since only a few materials have the exact total kinetic energy data carried away by the secondary particles in their library, NJOY computes KERMA factors by the energy-balance method [3]:

$$k_{ij}(E) = (E + Q_{ij} - \overline{E}_{ijn} - \overline{E}_{ijr})\sigma_{ij}(E), \tag{2}$$

where $\overline{E}_{ijn}$ and $\overline{E}_{ij\gamma}$ are the total energy of secondary neutron including multiplicity and that of photon including multiplicity, respectively. In the energy-balance method, the negative neutron heating may appear in some cases due to the inconsistent data set of neutron and photon. Even though the energy-balance method could induce unphysical negative values in the process, it is applicable to the heat calculation since the negative KERMA factors cancel the excess heating by photons and guarantee the conservation of total energy in large homogeneous system. Those pointwise KERMA factors are collapsed in the module GROUPR.

It is noted that the module GROUPR produces the neutron KERMA factors at infinite dilute condition. If these neutron KERMA factors were directly used in the heating calculation, the heat generation rate would be over-estimated because of unshielded cross sections. In order to account for the self-shielding in the neutron KERMA factor, the partial kinetic energy release per reaction is determined by dividing the partial KERMA factor by the neutron cross section and it is stored in the MC^2-3 library. In a MC^2-3 calculation, the neutron KERMA factors for a given composition are computed by multiplying the energy releases per reaction and self-shielded cross sections. Since the partial neutron KERMA factors are required to facilitate the self-shielding of neutron KERMA factors, the PreGAMMA code prepares an additional input of the HEATR module of NJOY. Table 2-1 shows the reactions and corresponding MT numbers considered in the PreGAMMA code to generate the neutron KERMA factor. When processing NJOY outputs using GenGAMMA, the obtained partial neutron KERMA factors are converted into the partial kinetic energy release per reaction. For the non-elastic reactions, the neutron KERMA factors computed by NJOY are directly given in the gamma library.

Table 2-1. Reaction Types Considered in PreGAMMA for Generation of Neutron KERMA Factors

MT number	Type of reaction
2	Elastic scattering
4	Inelastic scattering (Sum of the MT = 50-91)
18	Particle-induced fission
102	Radiative capture
103	Production of a proton (Sum of the MT = 600-649)
104	Production of a deuteron (Sum of the MT = 650-699)
105	Production of a triton (Sum of the MT = 700-749)
106	Production of a ^{3}He (Sum of the MT = 750-799)
107	Production of an alpha particle (Sum of the MT = 800-849)

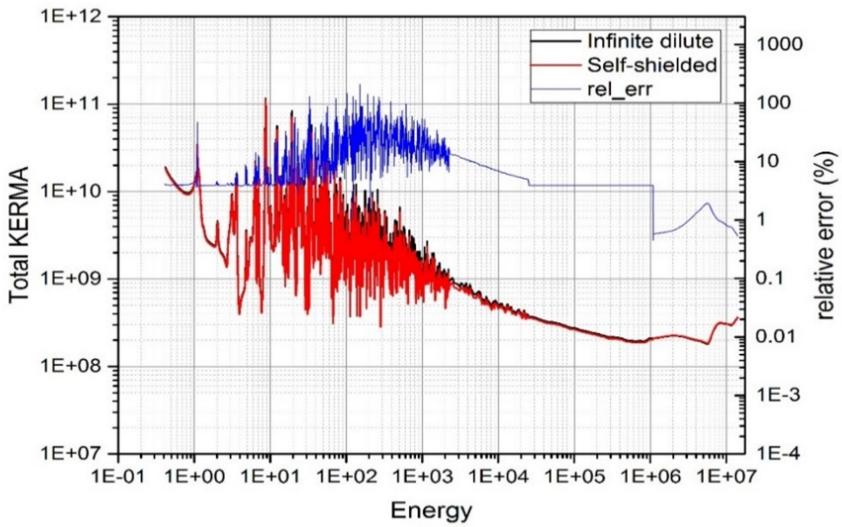

Figure 2-2. Self-shielded and Infinite Dilute Total Neutron KERMA Factor of U-235

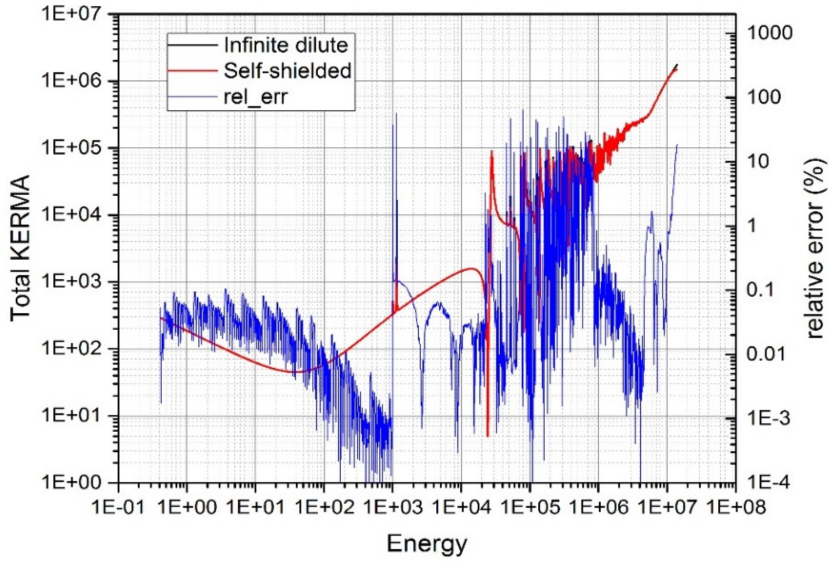

Figure 2-3. Self-shielded and Infinite Dilute Total Neutron KERMA Factor of Fe-56

For the ABTR fuel pin cell problem, 2,082 group KERMA factors were calculated with the infinite dilute and self-shielded cross sections. Figure 2-2 and Figure 2-3 compare these KERMA factors for ^{235}U and ^{56}Fe, respectively. The relative error indicates that the absolute value of relative error between two cross sections. As shown in Figure 2-2 and Figure 2-3, the relative errors of two KERMA factors become larger than 100% in the resonance energy range. Thus, the neglect of self-shielding effect on KERMA factor results in over-estimated heating rates in the resonance region.

2.4 Gamma Interaction Cross Section and KERMA Factors

The GAMINR module of NJOY provides cross sections for four different reactions from the ENDF photo-atomic sublibrary. The ENDF photo-atomic sublibrary includes the smooth cross section in File 23 in a similar way to the neutron cross section in File 3. Coherent, incoherent, pair production, and photoelectric cross sections and gamma KERMA factors are determined using the user-specified group structure and weighting spectrum. The module GAMINR provides a constant spectrum, 1/E spectrum and user-specified spectrum options to collapse the gamma interaction cross sections.

The PreGAMMA code prepares an input file of NJOY with a 1/E weighting spectrum with roll-offs since the 1/E weighting spectrum may represent the characteristics of gamma flux distribution in the core except for the low energy region below 0.1 MeV where the photoelectric absorption is dominant. In order to verify the adequacy of the 1/E weighting spectrum, 21-group gamma interaction cross sections of uranium were computed for the ABTR fuel pin mixture using NJOY with 1/E and constant spectra and compared with the MCNP6 reference results.

The relative statistical errors of MCNP6 results were less than 0.3% except for the high-energy region above 10 MeV. As shown in Figure 2-4, the cross sections computed with the 1/E spectrum agree well with the MCNP6 results except for the intermediate energy range where the relative errors show sharp peaks due to the gamma source from uranium and iron. Thus, it is judged that the 1/E spectrum is adequate to generate the base 94-group gamma library.

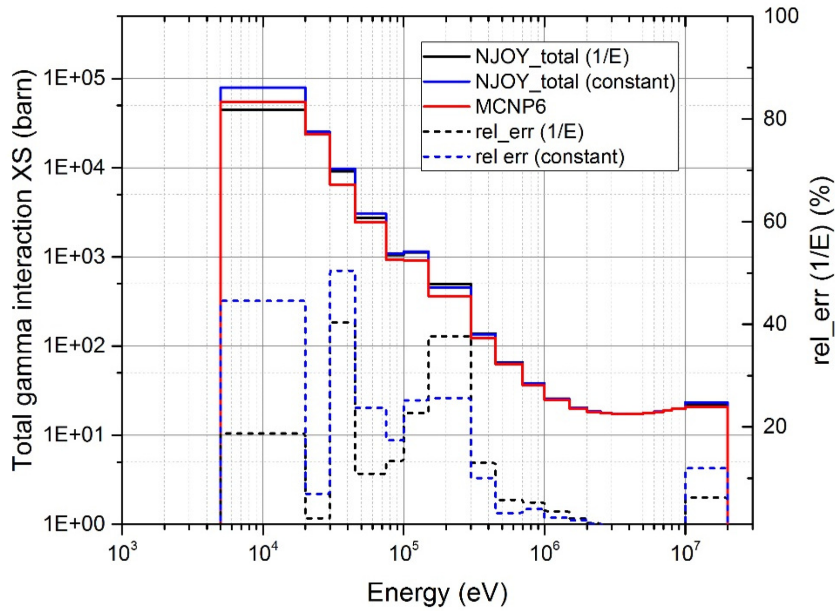

Figure 2-4. Total Gamma Interaction Cross Sections of Uranium in ABTR Fuel Pin Mixture

Since the mass of photon is negligible, the scattering of gamma ray is highly anisotropic. Thus, the Legendre scattering matrices were generated up to P_3 for the new 94-group gamma interaction cross section library. Note that the NJOY code should be modified to be able to handle 94 group gamma data, increasing the size of 'iamax' variable in the subroutine 'gaminr.f' up to 100,000.

In GenGAMMA, the gamma interaction cross sections and gamma KERMA factors in the GENDF file are directly employed in the new gamma library to be used in the gamma transport calculation of MC^2-3.

2.5 Delayed Photon Library

In the HEATR module of NJOY [3], the effective Q-value is determined by subtracting the portion of delayed photons and neutrinos from the mass difference Q-value. In order to obtain the exact KERMA factors and photon production matrix, the contribution of delayed photons should be considered after the process of NJOY. Main sources of delayed photons are the decays of fission products and their daughter isotopes. The contribution of delayed photons and betas resulting from the decay of fission products can be easily obtained from the ENDF data File 1, MT 458 that is based on the Sher's evaluation [7]. Under the assumption that beta particle energies are deposited locally at the site of fission occurred, the contribution of delayed betas to heat generation rates can be considered by adding the delayed beta KERMA factor to the total KERMA factor. The delayed beta KERMA factor can be determined by multiplying the total energy released by delayed betas with the self-shielded fission cross section.

For coupled neutron-gamma transport calculations, however, delayed gammas should be added to gamma production matrices. In the MC^2-2 code [8], the delayed gamma data were given in the DLYFIS file based on the ENDF/IV and those data were stored in the MCCF9 file, which is one of the MC^2-2 base library. The delayed gamma data in MCCF9 were no longer available in the MC^2-3 code, since the library MCCF9 has been replaced with the chi matrix and infinite-dilute UFG cross sections. In the ENDF/B VII.1 library, the delayed gamma source functions can be determined using the time constants in MT 460 of File 1 and the photon multiplicities in MT 460 of File 12. The delayed gamma source function is defined as the number of gammas emitted per unit time after the fission event, per unit energy for a fixed incident energy. Unfortunately, the yield data for delayed gamma are only given for ^{235}U and ^{239}Pu in the latest ENDF/B VII.1 library. Even though it reproduces the gamma ray spectra resulting from neutron-induced fission using 1,000 decay nuclides and 20,000 discrete-emission energies from England and Rider [9] and the NuDat nuclear database [10], the results are limited by the lack of experimental data and the uncertainties of fission product yields [11]. For these reasons, the PreGAMMA code calculates the delayed photon yield data using the latest decay and fission yield sublibraries. Users can specify the delayed photon production option in the "options" section of an input file of the PreGAMMA code. The delayed photon production option activates the calculation of delayed beta and delayed gamma yield from the ENDF-6 format library.

As mention above, the kinetic energies of delayed betas and gammas are retrieved from the ENDF/B File 1, MT 458. The energy components resulting from fission event in MT 458 can be expressed as [12]:

$$\begin{aligned} &E_i(E_{inc}) = E_i(0) - \delta E_i(E_{inc}) \qquad \text{if NPLY=0 }, \ \delta E_i(E_{inc}) = 0.075E_{inc} \\ &E_i(E_{inc}) = c_0 + \mathrm{c}_1\mathrm{E}_{inc} + \mathrm{c}_2\mathrm{E}_{inc}^2 \cdots \qquad \text{if NPLY} \neq 0 \end{aligned} \tag{3}$$

where NPLY indicates the order of polynomial expansion of the energy component, i is the index of energy component, E_{inc} is the incident neutron energy, $E_i(0)$ is a constant for delayed beta and gamma components of fission energy release, and $\delta E_i(E_{inc})$ is the function that defines the energy dependence of delayed beta and gamma energy components. The code reads these data to form the delayed photon library. In the MC^2-3 code, the contribution of delayed betas is determined by multiplying the energy component of delayed betas with the self-shielded fission cross section.

To calculate the delayed gamma production matrix, PreGAMMA constructs the decay chains of fission products by reading the fission yield and radioactive decay sublibraries. The gamma production matrix is then constructed by aggregating all the decay gamma spectra. The ENDF-6 format sublibraries of decay and fission yield provide the important information for decay heat analysis and fission products. The accuracy of delayed gamma yield calculation highly depends on the data in these libraries. The ENDF.B VII.1 and JENDL decay libraries are primarily based on the ENSDF (Evaluated Nuclear Structure Data File) [13], which includes evaluated nuclear structure and decay information obtained by international cooperation. Although the ENDF/B VII.1 sublibraries provide the decay data for all fission products, the accuracy of decay data are not guaranteed due to the incompleteness of experimental data for short-lived nuclides and complex decay scheme. Moreover, when the Q-value of a fission product increases, the gamma rays with weak energy are not observed in the gamma ray measurement. In order to overcome these inaccuracies in the decay heat analysis, the JENDL decay data was compiled in 2011 with the fission-product decay data file. To match the average beta and gamma decay energies with their spectral data, the JENDL decay data uses the theoretically calculated spectra and the total absorption gamma-ray spectroscopy (TAGS) data for the nuclides with incomplete decay scheme [14,15]. Therefore, the JENDL decay (JENDL/DDF-2015) and fission yield (JENDL/FPY-2011) data files [14] were used to generate the delayed gamma yield matrices in this report. In the PreGAMMA code, the summation of delayed gammas for each activation product is normalized to the average decay value using the theoretical spectrum.

Table 2-2 compares the delayed gamma energy per fission estimated by PreGAMMA using the fission yield and decay data of various libraries with the delayed gamma energy per fission in the File 1, MT 458 data of ENDF/B-VII.1. MCNP6 indicates the calculated delayed gamma energy using the decay data file of MCNP6 (CINDERGL.DAT) and ENDF/B VII.1 fission yield library. It can be seen that the delayed gamma energies estimated with the JENDL libraries agree with the MT 458 data better than the other libraries. In the PreGAMMA calculation, the delayed gamma production matrices are renormalized such that the total delayed gamma energy is equal to the reference value of MT 458 data.

Table 2-2. Specification of Cylindrical Fuel Pin Cell Model of ABTR

Fission Yield and Decay Libraries	^{235}U	^{238}U	^{239}Pu	^{240}Pu	^{241}Pu	^{242}Pu	^{241}Am
Reference (MT 458 of File 1)	6.33	8.25	5.17	6.49	6.40	6.82	5.51
ENDF/B VII.1	5.62	6.87	4.56	5.00	5.43	5.81	4.32
JENDL	6.22	7.72	5.25	5.77	6.27	6.65	5.02
Delayed Gamma Source Function (MT 460 of File 1)	2.90	-	2.99	-	-	-	-
MCNP6 (CINDERGL.DAT)	5.07	5.47	4.10	4.34	4.51	4.63	3.87

* Incident neutron energy = 0.0253 eV

3. Implementation of Gamma Transport Solver into MC²-3

The 0-D and 1-D gamma transport solvers were implemented into the MC²-3 code to perform the gamma transport calculation for group collapsing. The transport solver was developed by extending the existing driver routines for 0-D and 1-D transport calculations [1]. In the gamma transport calculation of MC²-3, the photoelectric absorption was treated as an absorption reaction in the gamma group constant. Note that the fluorescent effect, which is the emission of the portion of absorbed photon and electron from the photoelectric absorption, is not considered in the MC²-3 code yet. Incoherent (Compton) and coherent (Thompson) scatterings are treated as a simple scattering reaction, while the pair production reaction is treated as the (n,2n) reaction in the gamma transport calculation. If the gamma cross sections for individual regions are prepared, the transport calculation is performed with a fixed gamma source distribution. The fixed gamma source is calculated by multiplying the neutron flux with the gamma production matrices obtained from the neutron transport calculation. The following fixed-source gamma transport equation is solved using the 0-D and 1-D transport solver:

$$\Omega \cdot \nabla \phi_\gamma^g + \Sigma_t^g \phi_\gamma^g = \sum_{g'} \Sigma_{\gamma\gamma}^{g' \to g} \phi_\gamma^{g'} + \sum_n \Sigma_{\gamma n}^{n \to g} \phi_n^n + S_\gamma^g \qquad (4)$$

where the subscripts n and γ denote the neutron and gamma quantities, respectively, and the superscripts n and g represent the neutron and gamma groups, respectively. That is, ϕ_n^n is the n-th group neutron flux determined from the neutron transport calculation and ϕ_γ^g is the g-th group gamma flux. Σ_t^g is the macroscopic total cross section of gamma group g, $\Sigma_{\gamma\gamma}^{g' \to g}$ is the macroscopic scattering cross section from gamma group g' to g, $\Sigma_{\gamma n}^{n \to g}$ is the macroscopic production cross section from neutron group n to gamma group g, and S_γ^g represents the external gamma source.

The calculated gamma group flux is used in generating the broad-group gamma interaction cross sections and heating factors. For each broad group, the heating factor and interaction cross sections are determined by collapsing the 94-group cross sections in the library as

$$\sigma_x^G = \frac{\sum_{g \in G} \sigma_x^g \phi_\gamma^g}{\sum_{g \in G} \phi_\gamma^g}, \quad \sigma_x^{G' \to G} = \frac{\sum_{g \in G} \sum_{g' \in G'} \sigma_x^{g' \to g} \phi_\gamma^{g'}}{\sum_{g' \in G'} \phi_\gamma^{g'}} \qquad (5)$$

$$K_x^G = \frac{\sum_{g \in G} K_x^g \phi_\gamma^g}{\sum_{g \in G} \phi_\gamma^g} \qquad (6)$$

where σ and K represent the interaction cross section and gamma KERMA factor, respectively. The subscript x denotes the reaction type, and the superscript g and G denoting the fine and broad gamma group indices, respectively.

If the number of gamma groups in the library (input by *i_gammalibgroup*) is different from the number of broad groups requested (input by *c_gamma_structure*), a group collapsing is performed. Currently only two energy group structures as listed in Table 3-1 are available.

Table 3-1. MC^2-3 Inputs for Gamma Data Generation

$control

Name	Type	Option	Description
c_gamma_structure	Character (len=8)	ANL21G (D) ANL94G	Broad gamma group structure. Currently only ANL94G and ANLS 21G are available.
i_gammalibgroup	Integer	21 (D) 94	The number of gamma groups in the gamma library. If the number of gamma groups matches between c_gamma_structure and i_gammalibgroup, no group condensation is made.
l_delayed_gamma	Logical	True (D)	Use delayed gamma yield library if available for gamma production matrix. If false, the delayed gamma fission energy component in delayed photon library is used to generate PMATRX

* D: default

(Example)
To use the 94-group gamma library and generate the 21-group gamma data:

```
$control
…
l_gamma              = T
l_delayed_gamma      = T            ! default
c_gamma_structure    = ANL21G       ! default
i_gammalibgroup      = 94
/
```

To use the 94-group gamma library and generate the 94-group gamma data:

```
$control
…
l_gamma              = T
l_delayed_gamma      = T            ! default
c_gamma_structure    = ANL94G
i_gammalibgroup      = 94
/
```

To use the 21-group gamma library and generate the 21-group gamma data:

```
$control
…
l_gamma             = T
l_delayed_gamma     = T           ! default
c_gamma_structure   = ANL21G      ! default
i_gammalibgroup     = 21          ! default
/
```

Table 3-2. Built-in Gamma Multigroup Structures

ANL94G (CSEWG 94-group structure)

	1	2	3	4	5	6	7	8
1	2.0000E+07	1.4000E+07	1.2000E+07	1.1000E+07	1.0600E+07	1.0000E+07	9.5000E+06	9.0000E+06
9	8.5000E+06	8.0000E+06	7.7500E+06	7.5000E+06	7.2500E+06	7.0000E+06	6.7500E+06	6.5000E+06
17	6.2500E+06	6.0000E+06	5.7500E+06	5.5000E+06	5.4000E+06	5.2000E+06	5.0000E+06	4.7000E+06
25	4.5000E+06	4.4000E+06	4.2000E+06	4.0000E+06	3.9000E+06	3.8000E+06	3.6500E+06	3.5000E+06
33	3.3330E+06	3.1660E+06	3.0000E+06	2.8330E+06	2.6660E+06	2.5000E+06	2.3330E+06	2.1660E+06
41	2.0000E+06	1.8750E+06	1.7500E+06	1.6600E+06	1.6000E+06	1.5000E+06	1.4200E+06	1.3300E+06
49	1.2500E+06	1.2000E+06	1.1250E+06	1.0000E+06	9.0000E+05	8.6500E+05	8.2500E+05	8.0000E+05
57	7.5000E+05	7.0000E+05	6.7500E+05	6.5000E+05	6.2500E+05	6.0000E+05	5.7500E+05	5.5000E+05
65	5.2500E+05	5.0000E+05	4.5000E+05	4.2500E+05	4.0000E+05	3.7500E+05	3.5000E+05	3.2500E+05
73	3.0000E+05	2.6000E+05	2.2000E+05	1.9000E+05	1.6000E+05	1.5000E+05	1.4000E+05	1.2000E+05
81	1.0000E+05	9.0000E+04	8.0000E+04	7.5000E+04	6.5000E+04	6.0000E+04	5.5000E+04	4.5000E+04
89	4.0000E+04	3.5000E+04	3.0000E+04	2.0000E+04	1.5000E+04	1.0000E+04		

* Upper energy boundaries in eV are shown in the table.

ANL21G

	1	2	3	4	5	6	7	8
1	2.0000E+07	1.0000E+07	8.0000E+06	7.0000E+06	6.0000E+06	5.0000E+06	4.0000E+06	3.0000E+06
9	2.5000E+06	2.0000E+06	1.5000E+06	1.0000E+06	7.0000E+05	4.5000E+05	3.0000E+05	1.5000E+05
17	1.0000E+05	7.5000E+04	4.5000E+04	3.0000E+04	2.0000E+04			

* Upper energy boundaries in eV are shown in the table.

4. Verification Results

4.1 ABTR Fuel Pin Cell Calculation

As the first step to test the newly implemented gamma transport capabilities and libraries of MC^2-3, the gamma flux distribution and the gamma interaction cross sections were calculated for a cylindrical fuel pin problem of ABTR and compared with the reference MCNP6 solution. Both calculations were performed with the cross section libraries based on the ENDF/B VII.0 data. The MCNP6 calculation was performed with 1,000 active cycles and 10,000 histories per cycle. The delayed fission gammas were not considered since the MCNP6 cross section library lacks the corresponding data. The relative statistical errors of MCNP6 results were less than 0.3% except for the high-energy region above 10 MeV. The reflective boundary condition is imposed on the fuel pin boundary. Figure 4-1 shows the 94-group gamma flux distributions in the fuel region obtained from MC^2-3 calculations with and without delayed gammas and that from MCNP6 calculation without delayed gammas. It is clearly seen that the gamma flux distribution of MC^2-3 without delayed gammas agrees very well with the MCNP6 solution. Note that the sharp peak at 0.5 MeV is mainly due to the gamma rays from the neutron capture and fission reactions of U-235 and the pair production reactions in the high-energy range. The peak at 0.8 MeV is mainly due to the inelastic scattering reactions of Fe-56.

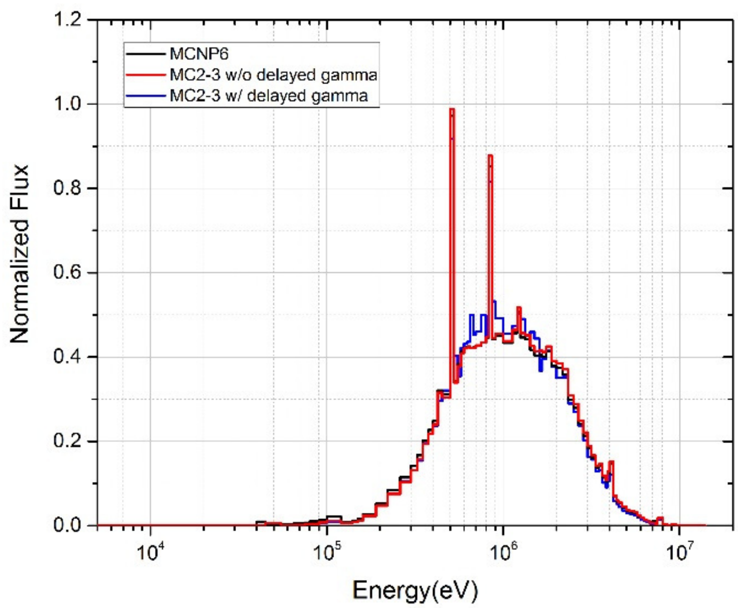

Figure 4-1. 94-group Gamma Flux Distributions for the ABTR Fuel Pin

Figure 4-2 and Figure 4-3 compare the 94- and 21-group total gamma interaction cross sections calculated with MC^2-3 and MCNP6 for uranium and iron, respectively. It can be seen that the 21-group gamma interaction cross sections determined with MC^2-3 agree very well with those determined with MCNP6 except for groups 17 to 19 (30 keV - 100 keV) and group 21 (5 keV – 20 keV). These differences in low-energy cross sections result from the differences in the 94-group gamma libraries themselves, which are caused by the abrupt changes in photoelectric absorption cross sections due to the absorption edges of different electron shells. These results indicate that the 94-group structure of CSEWG is not sufficiently fine to represent the photoelectric absorption edges accurately. However, as can be seen in Figure 4-2, the flux level is very low in the energy range below 100 keV, where the photoelectric absorption cross sections are important. Therefore, it is judged that the 94-group structure is adequate for the coupled neutron and gamma heating calculations.

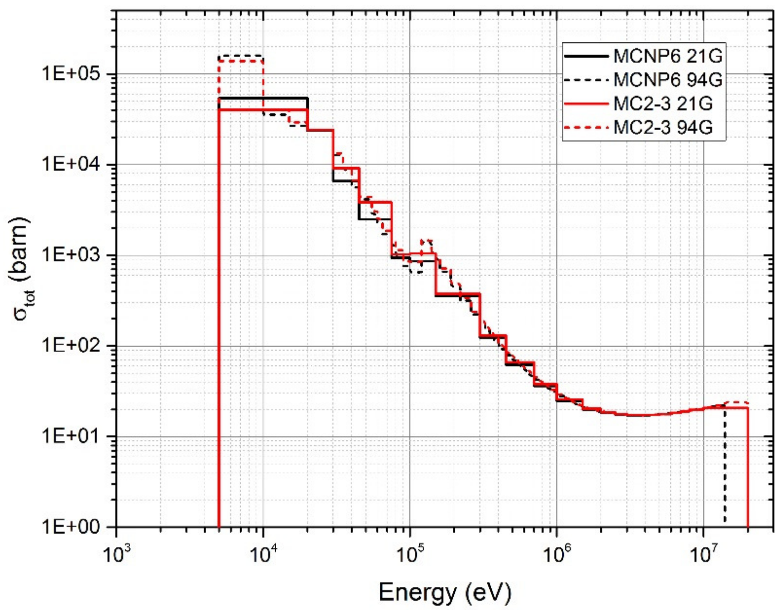

Figure 4-2. Total Gamma Cross Section of Uranium in the ABTR Fuel Pin

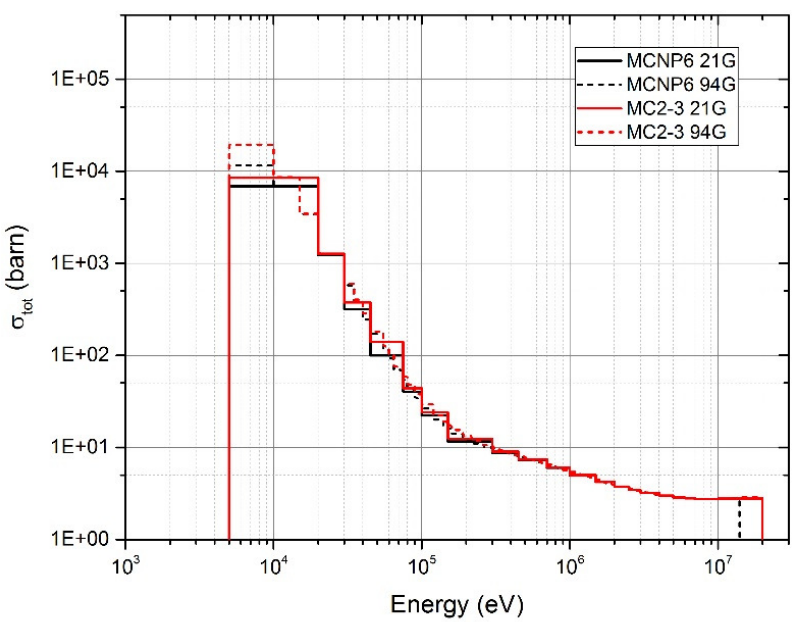

Figure 4-3. Total Gamma Cross Section of Iron in the ABTR Fuel Pin

4.2 EBR-II Run 132B Benchmark Problem

In order to examine the effects on power density, coupled neutron and gamma heating calculations were performed for the EBR-II benchmark problem [2] using DIF3D with the cross sections prepared with the new gamma data generation scheme of MC^2-3. The EBR-II benchmark problem is based on the core configuration of Run 132B, which consists of 71 regular driver fuel assemblies, 13 half-worth fuel driver assemblies, 10 control and safety assemblies, six structural assemblies, and six instrumented assemblies. The detailed core specifications can be found in References 2 and 16. Neutron and gamma cross section library was generated using the ENDF/B-VII.0 data. For comparison, a MCNP6 calculation was performed with 180 active cycles with 100,000 histories per cycle. The delayed fission gammas were not considered in both MC^2-3/VARIANT and MCNP6 calculations for a consistent comparison. The results of MCNP6 have relative statistical errors less than 0.2%.

Figure 4-4 shows the relative differences in assembly power of the DIF3D solution obtained with the new gamma data generation scheme of MC^2-3 from the MCNP6 solution. A set of 21-group gamma production and interaction cross sections were generated by MC^2-3 calculations with the new 94-group gamma library. As shown in Figure 4-4, the differences in assembly power from the MCNP6 solution are less than 4.1% by employing the new gamma library and gamma transport module of MC^2-3.

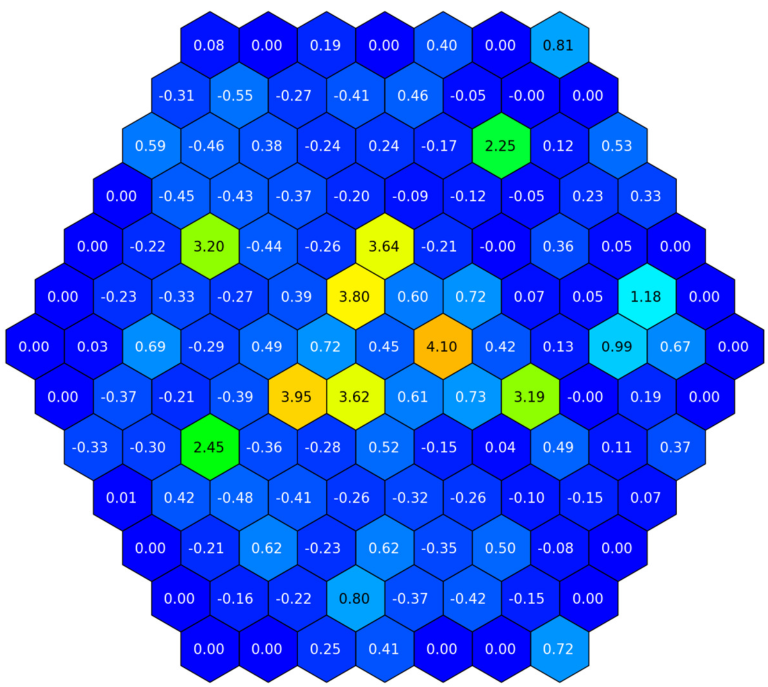

Figure 4-4. Relative Difference (%) in the Assembly Power Distribution between MCNP6 and DIF3D Using the 94-group Gamma Library

5. Input Description

5.1 Input File of PreGAMMA

A user input of PreGAMMA is composed of sections made by name cards. The following ten main sections can be defined: title, path of base libraries, path of the NJOY99 executable file, path of the GenGAMMA code, neutron cross section library, thermal scattering library, photo-atomic library, temperature, background cross section, neutron group structure, gamma group structure, and options. They are defined using the following name cards: TITLE, LIBRARY, NJOY99, GENDF, NUCLIDES, TSL, PHL, TEMPERATURE, BACKXS, GRSTR, GGRSTR, and OPTION. Every section should be made only once in a user input and starts with '{' and ends with '}'. The option section is composed of two sub-card commands, DELAYED_PHOTONS and GAMMA_LIBRARY. A slash, '/', is interpreted by the end of an input file. The format and description of individual sections are given below.

A. Title section

Name card	TITLE
Description	Title and the name of directory where output files will be stored

Format	TITLE
	{
	   title
	}

Variables	title (character, len=300)

B. Path of base libraries

Name card	LIBRARY
Description	Directories of the neutron cross section, thermal scattering, photo-atomic sublibraries

Format	LIBRARY
	{
	   dir1
	   dir2
	   dir3
	}

Variables	dir1 (character, len=300) : directory of the neutron cross section library dir2 (character, len=300) : directory of the thermal scattering library dir3 (character, len=300) : directory of the photo-atomic library

C. Path of the NJOY99 executable file

Name card	NJOY99
Description	Directory of the NJOY99 executable file
Format	NJOY99 { dir

	}
Variables	dir (character, len=300) : directory of the NJOY99 executable file (the NJOY99.396 version is highly recommended)

D. Path of the GenGAMMA code

Name card	GENDF
Description	Directory of the GenGAMMA code

Format	GENDF
	{
	dir
	}

Variables	dir (character, len=300) : directory of the GenGAMMA code executable file

E. Neutron cross section library

Name card	NUCLIDES
Description	File names of the neutron cross section libraries in the directory

Format 1	NUCLIDES
	{
	name1
	name2
	⋮
	}

Variables	name (character, len=300) : a file name of neutron cross section library for each nuclide

Format 2	NUCLIDES
	{
	ALL
	}

Sub-card	ALL : Read all neutron cross section libraries in the directory

F. Thermal scattering library

Name card	TSL
Description	(Optional : for the generation of thermal cross section library) File names of the thermal scattering libraries in the directory

Format	TSL
	{
	name1 nid1 tid1
	name2 nid2 tid2
	⋮
	}

Variables	name (character, len=80) : a file name of thermal scattering library for each nuclide nid (integer) : a ZA number of each nuclide ($ZA = 1000 \times Z + A$)

	tid (integer) : a ZA number of output file (arbitrary number)

G. Photoatomic library

Name card	PHL
Description	(Optional : for the generation of gamma library) File names of the photon-atomic libraries in the directory

Format	PHL
	{
	name1
	name2
	⋮
	}

Variables	name (character, len=80) : a file name of photo-atomic cross section library for each nuclide

H. Temperature

Name card	TEMP
Description	An array of temperatures

Format	TEMP
	{
	temp1 temp2 temp3 ⋯
	}

Variables	temp (real, dp) : a temperature in Kelvin

* Only one temperature is recommended, since GenGAMMA cannot handle multiple temperatures yet.

I. Background cross section

Name card	BACKXS
Description	An array of background cross sections

Format	BACKXS
	{
	xs1 xs2 xs3 ⋯
	}

Variables	xs (real, dp) : a background cross section in barn

* Only one background cross section is recommended, since GeGAMMA cannot handle multiple background cross sections yet.

J. Neutron group structure

Name card	GRSTR
Description	A number of neutron group, Legendre order and group structure
Format	GRSTR { gr lorder

	E_1 E_2 E_3 E_4 E_5 E_7 E_8 E_9 E_{10} E_{11} ⋮ E_{gr-3} E_{gr-2} E_{gr-1} E_{gr} E_{gr+1} }
Variables	gr (integer) : a number of neutron group lorder (integer) : a number of Legendre order E_i (real, dp) : lower energy bound of i-th energy group in eV

K. Gamma group structure

Name card	GGRSTR
Description	(Optional : for the generation of gamma library) A number of gamma group, Legendre order and group structure

Format	GGRSTR
	{
	gr lorder
	E_1 E_2 E_3 E_4 E_5
	E_7 E_8 E_9 E_{10} E_{11}
	⋮
	E_{gr-3} E_{gr-2} E_{gr-1} E_{gr} E_{gr+1}
	}

Variables	gr (integer) : a number of gamma group lorder (integer) : a number of Legendre order E_i (real, dp) : lower energy bound of i-th energy group in eV

L. Options

Name card	OPTION
Description	(Optional) The options for the MC^2-3 sublibrary generation

Format 1	OPTION
	{
	GAMMA_LIBRARY
	}

Sub-card	GAMMA_LIBRARY: generate prompt gamma production matrix, gamma interaction cross section and neutron and gamma KERMA factors for MC^2-3 gamma library

Format 2	OPTION
	{
	DELAYED_PHOTONS
	dir1
	dir2
	}

Sub-card	DELAYED_PHOTONS: generate delayed photon library and gamma yield matrix for MC^2-3 gamma library

Variables	dir1 (character, len=300) : directory of the decay sublibrary dir2 (character, len=300) : directory of the fission yield sublibrary

* Decay and fission yield sublibrary should be merged into one file, respectively.

5.2 Sample Inputs

```
TITLE
{
    ENDF/B-VII.1_Gamma_94
}
LIBRARY
{
    Z:\NJOY\NJOY.lib\n-ENDF-VII1.endf
    Z:\NJOY\NJOY.lib\tsl-ENDF-VII1.endf
    Z:\NJOY\NJOY.lib\photo-ENDF-VII1.endf
}
NJOY99
{
    /home/a/test/NJOY/NJOY.run/xnjoy99.396
}
GENDF
{
    /home/a/test/NJOY/njoy_tool/src/gendf.x
}
NUCLIDES
{
     n-001_H_001.endf
     n-008_O_016.endf
     n-092_U_235.endf
}
TSL
{
     tsl-HinH2O.endf    1001    1101
}
PHL
{
     photoat-001_H_000.endf
     photoat-008_O_000.endf
     photoat-092_U_000.endf
}
TEMP
{
    300
}
BACKXS
{
    1.0E+10
}
GRSTR
{
      2082    3
      4.14000E-01 4.17458E-01 4.20951E-01 4.24474E-01 4.28026E-01
```

```
                                                              ⋮
      1.33866E+07 1.34986E+07 1.36115E+07 1.37254E+07 1.38403E+07
      1.39561E+07 1.40729E+07 1.41907E+07
}
GGRSTR
{
    94    4
    5.00000E+03 1.00000E+04 1.50000E+04 2.00000E+04 3.00000E+04
                                                              ⋮
    1.06000E+07 1.10000E+07 1.20000E+07 1.40000E+07 2.00000E+07
}
OPTION
{
    DELAYED_PHOTONS
        Z:/NJOY/NJOY.lib/decay.jendl
        Z:/NJOY/NJOY.lib/nfy.jendl
    GAMMA_LIBRARY
}
/
```

Figure 5-1. Sample Input of PreGAMMA

The PreGAMMA code also generates the input file of the NJOY processing tool to form the sublibrary of MC^2-3. The general format of GenGAMMA is given in Table 5-1.

Table 5-1. Description of an Input File of GenGAMMA

Format	name1 matid1 lorder1 index1 name2 matid2 lorder2 index2 ⋮
Variables	name (character, len=80) : a file name of GENDF file for each nuclide matid (integer) : a MAT number for each nuclide lorder (integer) : a number of Legendre order index (integer) : an index of library processing 0 = prompt gamma production and neutron KERMA factor library 1 = gamma interaction cross section and gamma KERMA factor library 2 = thermal library

After a normal termination of the PreGAMMA code, the following files are stored in the subdirectory named with the string in TITLE card: input files of the NJOY code, an input file of NJOY output-processing tool, a batch file to run the NJOY code, and NJOY output-processing tool. Figure 5-2 through Figure 5-5 show these output files of PreGAMMA code.

```
moder /
   1  21
' 92-U -235 from ENDF/B-VII.1' /
  20 9228
0 /
reconr /
  21  22
' 92-U -235 from ENDF/B-VII.1' /
9228 /
 0.001 0.000 0.003 /
0 /
broadr /
  21  22  30
9228  1  0  1 0.000 /
 0.001 1.00E+06 0.003 /
  3.0000E+02
0 /
unresr /
  21  30  31
9228  1  1  1 /
  3.0000E+02
  1.0000E+10
0 /
heatr /
  21  31  32  50
9228 13  0  0  0  1 /
 302 304 316 318 402 403 404 405 406 407 442 443 444/
thermr /
   0  32  33
   0 9228  8  1  1  0  1  221  1
  3.0000E+02
 0.003  5.0017
groupr /
  21  33   0  40
9228  1  1  3  3  1  1  1
' 92-U -235 from ENDF/B-VII.1' /
 3.0000E+02
 1.0000E+10
 2082 /
 4.14000000E-01  4.17458000E-01  4.20951000E-01  4.24474000E-01
                                                          ⋮
  1.39561000E+07  1.40729000E+07  1.41907000E+07 /
  94 /
 5.00000000E+03  1.00000000E+04  1.50000000E+04  2.00000000E+04
                                                           ⋮
  1.20000000E+07  1.40000000E+07  2.00000000E+07 /
  3   1 /
  3   2 /
  3   4 /
  3 102 /
  3 221 /
  3 301 /
  3 302 /
  3 304 /
  3 402 /
  3 442 /
```

```
  3 443 /
  3 444 /
 16 102 /
 16  18 /
 17   3 /
  3 318 /
  3  18 /
  3 452 /
  3 455 /
  5 455 /
  6 /
  6 221 /
  0 /
  0 /
stop
```

Figure 5-2. Sample Input of NJOY for Generation of Prompt Gamma Production Matrix and Neutron KERMA Factor

```
moder /
   1  21
' 92-U -  0 from ENDF/B-VII.1' /
  20 9200
0 /
reconr /
  21  22
' 92-U -  0 from ENDF/B-VII.1' /
9200 /
 0.001 0.000 0.003 /
0 /
gaminr
  21  22   0  70
9200   1   3   4   1 /
' 92-U -  0 from ENDF/B-VII.1' /
  94 /
5.00000000E+03  1.00000000E+04  1.50000000E+04  2.00000000E+04
3.00000000E+04

:
1.06000000E+07  1.10000000E+07  1.20000000E+07  1.40000000E+07
2.00000000E+07
 -1  0 /
  0 /
stop
```

Figure 5-3. Sample input of NJOY for Generation of Gamma Interaction Cross Section and KERMA Factor

```
'  1001.gendf'  125 3 0
'  8016.gendf'  825 3 0
' 92235.gendf' 9228 3 0
'   100.gaminr'  100 4 1
'   800.gaminr'  800 4 1
'  9200.gaminr' 9200 4 1
```

Figure 5-4. Sample input of GenGAMMA

```
  echo " ===================================================="
  echo "                             1-H -  1   [  1/3]"
  echo " ===================================================="
cp
 /home/a/test/NJOY/NJOY.lib/n-ENDF-VII1.endf/n-001_H_001.endf tape20
 /home/a/test/NJOY/NJOY.run/xnjoy99.396 < 1001.inp
 mv tape40 ./out/1001.gendf
 rm -f tape* output

⋮

  echo " ===================================================="
  echo "                             1-H -  0   [  1/3]"
  echo " ===================================================="
cp
/home/a/test/NJOY/NJOY.lib/photo-ENDF-VII1.endf/photoat-001_H_000.endf
tape20
/home/a/test/NJOY/NJOY.run/xnjoy99.396 < 100_gaminr.inp
 mv tape70 ./out/100.gaminr
 rm -f tape* output

⋮

 cd ./out
 cp /home/a/test/NJOY/njoy_tool/src/gendf.x ./gendf.x
./gendf.x gendf_process.inp
```

Figure 5-5. Sample Batch File for NJOY

6. MC^2-3 Gamma Library Format

6.1 Prompt Gamma Production and Interaction Libraries

The prompt gamma production and interaction library is composed of two libraries: the prompt gamma production library, and the gamma interaction cross section library. The prompt gamma production library begins with a general information of library.

Table 6-1 and Table 6-2 show the structure of those libraries, and Figure 6-1, Figure 6-2, Figure 6-3, and Figure 6-4 in turn show examples of the prompt gamma production library, the gamma interaction cross section library, the delayed gamma and beta energy file, and the delayed gamma production file, respectively. In the library, each file contains heating or interaction cross section data of a single isotope. The table named “table_gammlib” includes the mapping of the files to isotopes, as shown in Appendix A.

Table 6-1. Structure of the Prompt Gamma Production Library

Number of repeated rows	Column 1	Column 2	Column 3	Column 4	Column 5	$\cdots$
1	Number of neutron group (Default:2082)	Number of gamma group (Default:94)	Number of gamma production group from capture (c)	Number of gamma production group from absorption (a)	Number of gamma production group from non-elastic (n)	-
2082	Neutron group index	Lower energy boundary	Upper energy boundary	-		
94	Gamma group index	Lower energy boundary	Upper energy boundary	-		
(c)	Neutron group index	Lower gamma group index (l)	Upper gamma group index (u)	$\sigma^{\gamma}_{n,cap}$	$\dfrac{\sigma^{\gamma}_{n,cap}}{\sigma_{n,cap}}$	$\dfrac{\sigma^{g,\gamma}_{n,cap}}{\sigma^{\gamma}_{n,cap}}$, $(g = l$ to u)
(a)	Neutron group index	Lower gamma group index (l)	Upper gamma group index (u)	$\sigma^{\gamma}_{n,abs}$	$\dfrac{\sigma^{\gamma}_{n,abs}}{\sigma_{n,abs}}$	$\dfrac{\sigma^{g,\gamma}_{n,abs}}{\sigma^{\gamma}_{n,abs}}$, $(g = l$ to u)
(n)	Neutron group index	Lower gamma group index (l)	Upper gamma group index (u)	$\sigma^{\gamma}_{n,nonels}$	1	$\dfrac{\sigma^{g,\gamma}_{n,nonels}}{\sigma^{\gamma}_{n,nonels}}$, $(g = l$ to u)
1	Comment ('kerma')	An array of the MT number for partial kinetic energy release (maximum 10 MT numbers)				
2082	Neutron group index	Lower energy boundary	Total KERMA factor	Partial kinetic energy release parameter corresponding to the MT number		
2082	Neutron group index	Total Damage factor	-			

* Note that n and g denotes the neutron and gamma groups, respectively, and $\sigma^{g,\gamma}_{n,rea}$ is the gamma production cross section for the neutron group n and gamma group g. $\sigma^{\gamma}_{n,rea}$ is the n-th group total gamma production cross section of the specific reaction and $\sigma_{n,rea}$ is the n-th group cross section for the specific reaction, respectively. Noted that the absorption reaction is defined as the summation of capture and fission reaction

Table 6-2. Structure of the Gamma Interaction Cross Section Library

Number of repeated rows	Column 1	Column 2	Column 3	Column 4	Column 5	⋯
1	Number of gamma group (Default:94)	Legendre order (Default:4)	-			
94	Gamma group index	Upper energy boundary	$\sigma_{g,i}$ (i = total, coherent, incoherent, pair production, absorption, KERMA)			
94	Lower gamma group index (l)	Upper gamma group index (u)	0^{th} moment total incoherent scattering cross section	$\sigma_{g\to g'}^{0,incoh}$, ($g' = l$ to u)		
94	Lower gamma group index (l)	Upper gamma group index (u)	1^{st} moment total incoherent scattering cross section	$\sigma_{g\to g'}^{1,incoh}$, ($g' = l$ to u)		
94	Lower gamma group index (l)	Upper gamma group index (u)	2^{nd} moment total incoherent scattering cross section	$\sigma_{g\to g'}^{2,incoh}$, ($g' = l$ to u)		
94	Lower gamma group index (l)	Upper gamma group index (u)	3^{rd} moment total incoherent scattering cross section	$\sigma_{g\to g'}^{3,incoh}$, ($g' = l$ to u)		

* Note than g denotes the gamma groups, and $\sigma_{g,i}$ is the microscopic cross section for specific reaction i or the total gamma KERMA factor. $\sigma_{g\to g'}^{L,incoh}$ is the L^{th} moment incoherent scattering matrix.

```
2082 94 1775 1775  839
neutron groups
 2082  4.14000E-01  4.17458E-01
 2081  4.17458E-01  4.20951E-01
 2080  4.20951E-01  4.24474E-01
…
gamma groups
   94  5.00000E+03  1.00000E+04
   93  1.00000E+04  1.50000E+04
   92  1.50000E+04  2.00000E+04
…
absorption
 2082    9   94  8.28400E+02    6.60453E+00  4.63033E-07  1.50486E-05  6.25098E-05  1.22704E-04 …
 2081    9   94  8.15855E+02    6.60786E+00  4.63337E-07  1.50585E-05  6.25507E-05  1.22785E-04 …
 2080    9   94  8.03650E+02    6.61111E+00  4.63632E-07  1.50681E-05  6.25906E-05  1.22863E-04 …
…
non-elastic
  839   93   93  2.88029E-05    1.00000E+00  2.88029E-05
  838   93   93  1.48540E-04    1.00000E+00  1.48540E-04
  837   93   93  2.74036E-04    1.00000E+00  2.74036E-04
…
kerma   5  443    2    4   18  102
 2082    4.17458E-01    1.91176E+10    1.36965E+08    3.53763E-03    0.00000E+00    1.69103E+08 …
 2081    4.20951E-01    1.88404E+10    1.36912E+08    3.56721E-03    0.00000E+00    1.69104E+08 …
 2080    4.24474E-01    1.85703E+10    1.36854E+08    3.59707E-03    0.00000E+00    1.69104E+08 …
…
damage energy production
 2082    4.17458E-01  7.66055E+05
 2081    4.20951E-01  7.54946E+05
 2080    4.24474E-01  7.44123E+05
 2079    4.28026E-01  7.33588E+05
…
```

Figure 6-1. Example of the Prompt Gamma Production Library (heatr_U235_7)

```
94 5
   94    1.00000E+04  1.39117E+05  2.41655E+03  1.48604E+01  0.00000E+00  1.36685E+05  …
   93    1.50000E+04  4.00618E+04  1.52372E+03  2.05804E+01  0.00000E+00  3.85175E+04  …
   92    2.00000E+04  2.92871E+04  9.54307E+02  2.48475E+01  0.00000E+00  2.83079E+04  …
…
(Note that below are the scattering data up to P4)
   94    94  1.480553E+01  1.480553E+01
   93    94  2.058039E+01  2.002982E+01  5.505676E-01
   92    93  2.484756E+01  2.296982E+01  1.877741E+00
   91    92  2.937719E+01  2.768283E+01  1.694360E+00
…
```

Figure 6-2. Example of the Gamma Interaction Cross Section Library (gaminr_U)

```
2082
total energy release of delayed beta
2082   6.500000E+06
2081   6.500000E+06
2080   6.500000E+06
…
total energy release of delayed gamma
2082   6.330000E+06
2081   6.330000E+06
2080   6.330000E+06
…
```

Figure 6-3. Example of the Delayed Gamma and Beta Energy File (dbeta_92235)

```
2082     94
   total multiplicity of delayed gamma
2082   1  94   0.000000E+00 7.862134E-08 5.025375E-07 7.631476E-07 4.842753E-06 9.837452E-06 …
2081   1  94   0.000000E+00 7.862134E-08 5.025375E-07 7.631476E-07 4.842753E-06 9.837452E-06 …
2080   1  94   0.000000E+00 7.862134E-08 5.025375E-07 7.631476E-07 4.842753E-06 9.837452E-06 …
…
```

Figure 6-4. Example of the Delayed Gamma Production File (dgamma_92235)

6.2 Delayed Photon Libraries

The delayed photon libraries include a library for delayed beta and gamma components of fission energy release and delayed gamma production library. Table 6-3 and Table 6-4 represent the structures of both libraries.

Table 6-3. Structure of the Delayed Beta and Gamma Energy Components Library

Number of repeated rows	Column 1	Column 2
1	Number of neutron group (Default:2082)	-
2082	Neutron group index	$\overline{E}_n^{dly,\beta}$
2082	Neutron group index	$\overline{E}_n^{dly,\gamma}$

* $\overline{E}_n^{dly,pho}$ is the multigroup energy release component of delayed photon from a fission event.

Table 6-4. Structure of the Delayed Gamma Production Library

Number of repeated rows	Column 1	Column 2	Column 3	…
1	Number of neutron group (Default:2082)	Number of neutron group (Default:94)	-	
2082	Neutron group index	Lower gamma group index (l)	Upper gamma group index (u)	$y_n^{g,dly\ \gamma}, (g = l\ to\ u)$

* $y_n^{g,dly\ \gamma}$ indicates the delayed gamma production yield of n-th neutron group and g-th gamma group.

7. Summary

In order to improve the gamma heating accuracy for the coupled neutron-gamma transport calculation, the gamma yield and interaction cross section libraries were generated in the 94-group gamma structure, developing the newly developed PreGAMMA code and updating the GenGAMMA code. A new computational scheme for gamma data generation was implemented in MC^2-3. A module for gamma transport calculation was also implemented in MC^2-3 in order to calculate the 94-group gamma flux distribution used as the weighting spectrum for the generation of broad-group gamma cross sections.

The new capabilities of MC^2-3 for gamma cross section generation were tested using an ABTR fuel pin problem and the EBR-II benchmark problem. Detailed comparison of gamma spectra and gamma interaction cross sections for the ABTR pin cell problem showed that the MC^2-3 results agree well with the corresponding MCNP6 results except for the low energy range where the photoelectric absorption reaction is dominant and the gamma flux level is very low. From the coupled neutron and gamma heating calculation with DIF3D for the EBR-II benchmark problem, it was observed that the assembly powers obtained with the new gamma cross sections agree well with the MCNP6 results within 4.1%.

This document provides the input descriptions and examples for the PreGAMMA (preparing NJOY inputs and generating delayed gamma and betas) and GenGAMMA (processing NJOY outputs to generate the gamma library) codes as well as the data structure of the new 94-group gamma library.

References

1. C. H. Lee and W. S. Yang, “MC^2-3 : Multigroup Cross Section Generation Code for Fast Reactor Analysis Nuclear,” ANL/NE-11-41, Rev. 3, August 31, 2018.
2. T. Fei, C. H. Lee, T. K. Kim, and T. Sofu, “Calculation of Photon Heat Generation for EBR-II Using DIF3D/MC^2-3,” *Trans. Am. Nucl. Soc.*, **106**, 711 (2012).
3. R. E. MacFarlane and D. W. Muir, “NJOY99.0: Code System for Producing Pointwise and Multigroup Neutron and Photon Cross Sections from ENDF/B Data,” PSR-480/NJOY99.0, Oak Ridge National Laboratory (2000).
4. G. Palmiotti, E. E. Lewis, and C. B. Carrico, “VARIANT: VARIational Anisotropic Nodal Transport for Multidimensional Cartesian and Hexagonal Geometry Calculation,” ANL-95/40, Argonne National Laboratory (1995).
5. J. T. Goorley, et al., “Initial MCNP6 Release Overview - MCNP6 Version 1.0," LA-UR-13-22934, Los Alamos National Laboratory (2013).
6. W. S. Yang, T. K. Kim, and R. N. Hill, “Core Design Studies for Advanced Burner Test Reactor,” *Proc. of ICAPP 2007*, Nice Acropolis, France, May 13-18, 2007.
7. R. Sher and C. Beck, “Fission Energy Release for 16 Fissioning Nuclides,” EPRI-NP-1771, Electric Power Research Institute (1981).
8. C. G. S. H. Henryson, II, B. J. Toppel, “MC^2-2: A Code to Calculate Fast Neutron Spectra and Multigroup Cross Sections,” ANL-8144, Argonne National Laboratory (1976).
9. T. England and B. Rider, “Evaluation and Compilation of Fission Product Yields”, LA-UR-94-3106, ENDF-349, Lawrence Livermore National Laboratory (1994).
10. National Nuclear Data Center, http://www.nndc.bnl.gov/nudat2/.
11. J. M. Hall, J. A. Pruet, D. A. Brown, M. A. Descalle, G. W. Hedstrom, and S. G. Prussin, “Modeling the Production of Beta-Delayed Gamma Rays for the Detection of Special Nuclear Materials,” UCRL-TR-209738, Lawrence Livermore National Laboratory (2005).
12. A. Trkov, M. Herman, and D. Brown, “"ENDF-6 Formats Manual: Data Formats and Procedures for the Evaluated Nuclear Data Files ENDF/B-VI and ENDF/B-VII,” ENDF-102, National Nuclear Data Center, Brookhaven National Laboratory (2012).
13. J. K. Tuli, “Evaluated Nuclear Structure Data File, A Manual for Preparation of Data Sets," BNL-NCS-51655-01/02-Rev, National Nuclear Data Center, Brookhaven National Laboratory (2001).
14. J. I. Katakura, T. Yoshida, K. Oyamatsu, and T. Tachibana, “Estimation of beta- and gamma-ray spectra for JENDL FP decay data file,” *J. Nucl. Sci. Technol.*, **38**, 470 (2001).
15. J. Katakura, “JENDL FP Decay Data File 2011 and Fission Yields Data File 2011,” JAEA-Data/Code 2011-025, Japan Atomic Energy Agency (2012).
16. L. L. Briggs, T. Sumner, T. Fei, T. Sofu, and S. Monti, “EBR-II Passive Safety Demonstration Tests Benchmark Analyses – Phase 1,” *Trans. Am. Nucl. Soc.*, **111**, 1263 (2014).

Appendix A. MC²-3 Gamma Library Table for ENDF/B-VII.0 Data

table_gammalib

```
393
1    2 H1___7   heatr_H_001      gaminr_H
2    2 H2___7   heatr_H_002      gaminr_H
3    2 H3___7   heatr_H_003      gaminr_H
4    2 HE3__7   heatr_He_003     gaminr_He
5    2 HE4__7   heatr_He_004     gaminr_He
6    2 LI6__7   heatr_Li_006     gaminr_Li
7    2 LI7__7   heatr_Li_007     gaminr_Li
8    2 BE7__7   heatr_Be_007     gaminr_Be
9    2 BE9__7   heatr_Be_009     gaminr_Be
10   2 B10__7   heatr_B_010      gaminr_B
11   2 B11__7   heatr_B_011      gaminr_B
12   2 C____7   heatr_C_000      gaminr_C
13   2 N14__7   heatr_N_014      gaminr_N
14   2 N15__7   heatr_N_015      gaminr_N
15   2 O16__7   heatr_O_016      gaminr_O
16   2 O17__7   heatr_O_017      gaminr_O
17   2 F19__7   heatr_F_019      gaminr_F
18   2 NA22_7   heatr_Na_022     gaminr_Na
19   2 NA23_7   heatr_Na_023     gaminr_Na
20   2 MG24_7   heatr_Mg_024     gaminr_Mg
21   2 MG25_7   heatr_Mg_025     gaminr_Mg
22   2 MG26_7   heatr_Mg_026     gaminr_Mg
23   2 AL27_7   heatr_Al_027     gaminr_Al
24   2 SI28_7   heatr_Si_028     gaminr_Si
25   2 SI29_7   heatr_Si_029     gaminr_Si
26   2 SI30_7   heatr_Si_030     gaminr_Si
27   2 P31__7   heatr_P_031      gaminr_P
28   2 S32__7   heatr_S_032      gaminr_S
29   2 S33__7   heatr_S_033      gaminr_S
30   2 S34__7   heatr_S_034      gaminr_S
31   2 S36__7   heatr_S_036      gaminr_S
32   2 CL35_7   heatr_Cl_035     gaminr_Cl
33   2 CL37_7   heatr_Cl_037     gaminr_Cl
34   2 AR36_7   heatr_Ar_036     gaminr_Ar
35   2 AR38_7   heatr_Ar_038     gaminr_Ar
36   2 AR40_7   heatr_Ar_040     gaminr_Ar
37   2 K39__7   heatr_K_039      gaminr_K
38   2 K40__7   heatr_K_040      gaminr_K
39   2 K41__7   heatr_K_041      gaminr_K
40   2 CA40_7   heatr_Ca_040     gaminr_Ca
41   2 CA42_7   heatr_Ca_042     gaminr_Ca
42   2 CA43_7   heatr_Ca_043     gaminr_Ca
43   2 CA44_7   heatr_Ca_044     gaminr_Ca
44   2 CA46_7   heatr_Ca_046     gaminr_Ca
45   2 CA48_7   heatr_Ca_048     gaminr_Ca
46   2 SC45_7   heatr_Sc_045     gaminr_Sc
47   2 TI46_7   heatr_Ti_046     gaminr_Ti
48   2 TI47_7   heatr_Ti_047     gaminr_Ti
49   2 TI48_7   heatr_Ti_048     gaminr_Ti
50   2 TI49_7   heatr_Ti_049     gaminr_Ti
51   2 TI50_7   heatr_Ti_050     gaminr_Ti
52   2 V____7   heatr_V_000      gaminr_V
53   2 CR50_7   heatr_Cr_050     gaminr_Cr
54   2 CR52_7   heatr_Cr_052     gaminr_Cr
55   2 CR53_7   heatr_Cr_053     gaminr_Cr
56   2 CR54_7   heatr_Cr_054     gaminr_Cr
```

```
57  2 MN55_7   heatr_Mn_055     gaminr_Mn
58  2 FE54_7   heatr_Fe_054     gaminr_Fe
59  2 FE56_7   heatr_Fe_056     gaminr_Fe
60  2 FE57_7   heatr_Fe_057     gaminr_Fe
61  2 FE58_7   heatr_Fe_058     gaminr_Fe
62  2 CO58_7   heatr_Co_058     gaminr_Co
63  2 CO58M7   heatr_Co_058m1   gaminr_Co
64  2 CO59_7   heatr_Co_059     gaminr_Co
65  2 NI58_7   heatr_Ni_058     gaminr_Ni
66  2 NI59_7   heatr_Ni_059     gaminr_Ni
67  2 NI60_7   heatr_Ni_060     gaminr_Ni
68  2 NI61_7   heatr_Ni_061     gaminr_Ni
69  2 NI62_7   heatr_Ni_062     gaminr_Ni
70  2 NI64_7   heatr_Ni_064     gaminr_Ni
71  2 CU63_7   heatr_Cu_063     gaminr_Cu
72  2 CU65_7   heatr_Cu_065     gaminr_Cu
73  2 ZN___7   heatr_Zn_000     gaminr_Zn
74  2 GA69_7   heatr_Ga_069     gaminr_Ga
75  2 GA71_7   heatr_Ga_071     gaminr_Ga
76  2 GE70_7   heatr_Ge_070     gaminr_Ge
77  2 GE72_7   heatr_Ge_072     gaminr_Ge
78  2 GE73_7   heatr_Ge_073     gaminr_Ge
79  2 GE74_7   heatr_Ge_074     gaminr_Ge
80  2 GE76_7   heatr_Ge_076     gaminr_Ge
81  2 AS74_7   heatr_As_074     gaminr_As
82  2 AS75_7   heatr_As_075     gaminr_As
83  2 SE74_7   heatr_Se_074     gaminr_Se
84  2 SE76_7   heatr_Se_076     gaminr_Se
85  2 SE77_7   heatr_Se_077     gaminr_Se
86  2 SE78_7   heatr_Se_078     gaminr_Se
87  2 SE79_7   heatr_Se_079     gaminr_Se
88  2 SE80_7   heatr_Se_080     gaminr_Se
89  2 SE82_7   heatr_Se_082     gaminr_Se
90  2 BR79_7   heatr_Br_079     gaminr_Br
91  2 BR81_7   heatr_Br_081     gaminr_Br
92  2 KR78_7   heatr_Kr_078     gaminr_Kr
93  2 KR80_7   heatr_Kr_080     gaminr_Kr
94  2 KR82_7   heatr_Kr_082     gaminr_Kr
95  2 KR83_7   heatr_Kr_083     gaminr_Kr
96  2 KR84_7   heatr_Kr_084     gaminr_Kr
97  2 KR85_7   heatr_Kr_085     gaminr_Kr
98  2 KR86_7   heatr_Kr_086     gaminr_Kr
99  2 RB85_7   heatr_Rb_085     gaminr_Rb
100 2 RB86_7   heatr_Rb_086     gaminr_Rb
101 2 RB87_7   heatr_Rb_087     gaminr_Rb
102 2 SR84_7   heatr_Sr_084     gaminr_Sr
103 2 SR86_7   heatr_Sr_086     gaminr_Sr
104 2 SR87_7   heatr_Sr_087     gaminr_Sr
105 2 SR88_7   heatr_Sr_088     gaminr_Sr
106 2 SR89_7   heatr_Sr_089     gaminr_Sr
107 2 SR90_7   heatr_Sr_090     gaminr_Sr
108 2 Y89__7   heatr_Y_089      gaminr_Y
109 2 Y90__7   heatr_Y_090      gaminr_Y
110 2 Y91__7   heatr_Y_091      gaminr_Y
111 2 ZR90_7   heatr_Zr_090     gaminr_Zr
112 2 ZR91_7   heatr_Zr_091     gaminr_Zr
113 2 ZR92_7   heatr_Zr_092     gaminr_Zr
114 2 ZR93_7   heatr_Zr_093     gaminr_Zr
115 2 ZR94_7   heatr_Zr_094     gaminr_Zr
116 2 ZR95_7   heatr_Zr_095     gaminr_Zr
117 2 ZR96_7   heatr_Zr_096     gaminr_Zr
```

```
118 2 NB93_7   heatr_Nb_093    gaminr_Nb
119 2 NB94_7   heatr_Nb_094    gaminr_Nb
120 2 NB95_7   heatr_Nb_095    gaminr_Nb
121 2 MO92_7   heatr_Mo_092    gaminr_Mo
122 2 MO94_7   heatr_Mo_094    gaminr_Mo
123 2 MO95_7   heatr_Mo_095    gaminr_Mo
124 2 MO96_7   heatr_Mo_096    gaminr_Mo
125 2 MO97_7   heatr_Mo_097    gaminr_Mo
126 2 MO98_7   heatr_Mo_098    gaminr_Mo
127 2 MO99_7   heatr_Mo_099    gaminr_Mo
128 2 MO1007   heatr_Mo_100    gaminr_Mo
129 2 TC99_7   heatr_Tc_099    gaminr_Tc
130 2 RU96_7   heatr_Ru_096    gaminr_Ru
131 2 RU98_7   heatr_Ru_098    gaminr_Ru
132 2 RU99_7   heatr_Ru_099    gaminr_Ru
133 2 RU1007   heatr_Ru_100    gaminr_Ru
134 2 RU1017   heatr_Ru_101    gaminr_Ru
135 2 RU1027   heatr_Ru_102    gaminr_Ru
136 2 RU1037   heatr_Ru_103    gaminr_Ru
137 2 RU1047   heatr_Ru_104    gaminr_Ru
138 2 RU1057   heatr_Ru_105    gaminr_Ru
139 2 RU1067   heatr_Ru_106    gaminr_Ru
140 2 RH1037   heatr_Rh_103    gaminr_Rh
141 2 RH1057   heatr_Rh_105    gaminr_Rh
142 2 PD1027   heatr_Pd_102    gaminr_Pd
143 2 PD1047   heatr_Pd_104    gaminr_Pd
144 2 PD1057   heatr_Pd_105    gaminr_Pd
145 2 PD1067   heatr_Pd_106    gaminr_Pd
146 2 PD1077   heatr_Pd_107    gaminr_Pd
147 2 PD1087   heatr_Pd_108    gaminr_Pd
148 2 PD1107   heatr_Pd_110    gaminr_Pd
149 2 AG1077   heatr_Ag_107    gaminr_Ag
150 2 AG1097   heatr_Ag_109    gaminr_Ag
151 2 AG10M7   heatr_Ag_110m1  gaminr_Ag
152 2 AG1117   heatr_Ag_111    gaminr_Ag
153 2 CD1067   heatr_Cd_106    gaminr_Cd
154 2 CD1087   heatr_Cd_108    gaminr_Cd
155 2 CD1107   heatr_Cd_110    gaminr_Cd
156 2 CD1117   heatr_Cd_111    gaminr_Cd
157 2 CD1127   heatr_Cd_112    gaminr_Cd
158 2 CD1137   heatr_Cd_113    gaminr_Cd
159 2 CD1147   heatr_Cd_114    gaminr_Cd
160 2 CD15M7   heatr_Cd_115m1  gaminr_Cd
161 2 CD1167   heatr_Cd_116    gaminr_Cd
162 2 IN1137   heatr_In_113    gaminr_In
163 2 IN1157   heatr_In_115    gaminr_In
164 2 SN1127   heatr_Sn_112    gaminr_Sn
165 2 SN1137   heatr_Sn_113    gaminr_Sn
166 2 SN1147   heatr_Sn_114    gaminr_Sn
167 2 SN1157   heatr_Sn_115    gaminr_Sn
168 2 SN1167   heatr_Sn_116    gaminr_Sn
169 2 SN1177   heatr_Sn_117    gaminr_Sn
170 2 SN1187   heatr_Sn_118    gaminr_Sn
171 2 SN1197   heatr_Sn_119    gaminr_Sn
172 2 SN1207   heatr_Sn_120    gaminr_Sn
173 2 SN1227   heatr_Sn_122    gaminr_Sn
174 2 SN1237   heatr_Sn_123    gaminr_Sn
175 2 SN1247   heatr_Sn_124    gaminr_Sn
176 2 SN1257   heatr_Sn_125    gaminr_Sn
177 2 SN1267   heatr_Sn_126    gaminr_Sn
178 2 SB1217   heatr_Sb_121    gaminr_Sb
```

```
179 2 SB1237   heatr_Sb_123     gaminr_Sb
180 2 SB1247   heatr_Sb_124     gaminr_Sb
181 2 SB1257   heatr_Sb_125     gaminr_Sb
182 2 SB1267   heatr_Sb_126     gaminr_Sb
183 2 TE1207   heatr_Te_120     gaminr_Te
184 2 TE1227   heatr_Te_122     gaminr_Te
185 2 TE1237   heatr_Te_123     gaminr_Te
186 2 TE1247   heatr_Te_124     gaminr_Te
187 2 TE1257   heatr_Te_125     gaminr_Te
188 2 TE1267   heatr_Te_126     gaminr_Te
189 2 TE27M7   heatr_Te_127m1   gaminr_Te
190 2 TE1287   heatr_Te_128     gaminr_Te
191 2 TE29M7   heatr_Te_129m1   gaminr_Te
192 2 TE1307   heatr_Te_130     gaminr_Te
193 2 TE1327   heatr_Te_132     gaminr_Te
194 2 I127_7   heatr_I_127      gaminr_I
195 2 I129_7   heatr_I_129      gaminr_I
196 2 I130_7   heatr_I_130      gaminr_I
197 2 I131_7   heatr_I_131      gaminr_I
198 2 I135_7   heatr_I_135      gaminr_I
199 2 XE1237   heatr_Xe_123     gaminr_Xe
200 2 XE1247   heatr_Xe_124     gaminr_Xe
201 2 XE1267   heatr_Xe_126     gaminr_Xe
202 2 XE1287   heatr_Xe_128     gaminr_Xe
203 2 XE1297   heatr_Xe_129     gaminr_Xe
204 2 XE1307   heatr_Xe_130     gaminr_Xe
205 2 XE1317   heatr_Xe_131     gaminr_Xe
206 2 XE1327   heatr_Xe_132     gaminr_Xe
207 2 XE1337   heatr_Xe_133     gaminr_Xe
208 2 XE1347   heatr_Xe_134     gaminr_Xe
209 2 XE1357   heatr_Xe_135     gaminr_Xe
210 2 XE1367   heatr_Xe_136     gaminr_Xe
211 2 CS1337   heatr_Cs_133     gaminr_Cs
212 2 CS1347   heatr_Cs_134     gaminr_Cs
213 2 CS1357   heatr_Cs_135     gaminr_Cs
214 2 CS1367   heatr_Cs_136     gaminr_Cs
215 2 CS1377   heatr_Cs_137     gaminr_Cs
216 2 BA1307   heatr_Ba_130     gaminr_Ba
217 2 BA1327   heatr_Ba_132     gaminr_Ba
218 2 BA1337   heatr_Ba_133     gaminr_Ba
219 2 BA1347   heatr_Ba_134     gaminr_Ba
220 2 BA1357   heatr_Ba_135     gaminr_Ba
221 2 BA1367   heatr_Ba_136     gaminr_Ba
222 2 BA1377   heatr_Ba_137     gaminr_Ba
223 2 BA1387   heatr_Ba_138     gaminr_Ba
224 2 BA1407   heatr_Ba_140     gaminr_Ba
225 2 LA1387   heatr_La_138     gaminr_La
226 2 LA1397   heatr_La_139     gaminr_La
227 2 LA1407   heatr_La_140     gaminr_La
228 2 CE1367   heatr_Ce_136     gaminr_Ce
229 2 CE1387   heatr_Ce_138     gaminr_Ce
230 2 CE1397   heatr_Ce_139     gaminr_Ce
231 2 CE1407   heatr_Ce_140     gaminr_Ce
232 2 CE1417   heatr_Ce_141     gaminr_Ce
233 2 CE1427   heatr_Ce_142     gaminr_Ce
234 2 CE1437   heatr_Ce_143     gaminr_Ce
235 2 CE1447   heatr_Ce_144     gaminr_Ce
236 2 PR1417   heatr_Pr_141     gaminr_Pr
237 2 PR1427   heatr_Pr_142     gaminr_Pr
238 2 PR1437   heatr_Pr_143     gaminr_Pr
239 2 ND1427   heatr_Nd_142     gaminr_Nd
```

```
240 2 ND1437   heatr_Nd_143     gaminr_Nd
241 2 ND1447   heatr_Nd_144     gaminr_Nd
242 2 ND1457   heatr_Nd_145     gaminr_Nd
243 2 ND1467   heatr_Nd_146     gaminr_Nd
244 2 ND1477   heatr_Nd_147     gaminr_Nd
245 2 ND1487   heatr_Nd_148     gaminr_Nd
246 2 ND1507   heatr_Nd_150     gaminr_Nd
247 2 PM1477   heatr_Pm_147     gaminr_Pm
248 2 PM1487   heatr_Pm_148     gaminr_Pm
249 2 PM48M7   heatr_Pm_148m1   gaminr_Pm
250 2 PM1497   heatr_Pm_149     gaminr_Pm
251 2 PM1517   heatr_Pm_151     gaminr_Pm
252 2 SM1447   heatr_Sm_144     gaminr_Sm
253 2 SM1477   heatr_Sm_147     gaminr_Sm
254 2 SM1487   heatr_Sm_148     gaminr_Sm
255 2 SM1497   heatr_Sm_149     gaminr_Sm
256 2 SM1507   heatr_Sm_150     gaminr_Sm
257 2 SM1517   heatr_Sm_151     gaminr_Sm
258 2 SM1527   heatr_Sm_152     gaminr_Sm
259 2 SM1537   heatr_Sm_153     gaminr_Sm
260 2 SM1547   heatr_Sm_154     gaminr_Sm
261 2 EU1517   heatr_Eu_151     gaminr_Eu
262 2 EU1527   heatr_Eu_152     gaminr_Eu
263 2 EU1537   heatr_Eu_153     gaminr_Eu
264 2 EU1547   heatr_Eu_154     gaminr_Eu
265 2 EU1557   heatr_Eu_155     gaminr_Eu
266 2 EU1567   heatr_Eu_156     gaminr_Eu
267 2 EU1577   heatr_Eu_157     gaminr_Eu
268 2 GD1527   heatr_Gd_152     gaminr_Gd
269 2 GD1537   heatr_Gd_153     gaminr_Gd
270 2 GD1547   heatr_Gd_154     gaminr_Gd
271 2 GD1557   heatr_Gd_155     gaminr_Gd
272 2 GD1567   heatr_Gd_156     gaminr_Gd
273 2 GD1577   heatr_Gd_157     gaminr_Gd
274 2 GD1587   heatr_Gd_158     gaminr_Gd
275 2 GD1607   heatr_Gd_160     gaminr_Gd
276 2 TB1597   heatr_Tb_159     gaminr_Tb
277 2 TB1607   heatr_Tb_160     gaminr_Tb
278 2 DY1567   heatr_Dy_156     gaminr_Dy
279 2 DY1587   heatr_Dy_158     gaminr_Dy
280 2 DY1607   heatr_Dy_160     gaminr_Dy
281 2 DY1617   heatr_Dy_161     gaminr_Dy
282 2 DY1627   heatr_Dy_162     gaminr_Dy
283 2 DY1637   heatr_Dy_163     gaminr_Dy
284 2 DY1647   heatr_Dy_164     gaminr_Dy
285 2 HO1657   heatr_Ho_165     gaminr_Ho
286 2 HO66M7   heatr_Ho_166m1   gaminr_Ho
287 2 ER1627   heatr_Er_162     gaminr_Er
288 2 ER1647   heatr_Er_164     gaminr_Er
289 2 ER1667   heatr_Er_166     gaminr_Er
290 2 ER1677   heatr_Er_167     gaminr_Er
291 2 ER1687   heatr_Er_168     gaminr_Er
292 2 ER1707   heatr_Er_170     gaminr_Er
293 2 LU1757   heatr_Lu_175     gaminr_Lu
294 2 LU1767   heatr_Lu_176     gaminr_Lu
295 2 HF1747   heatr_Hf_174     gaminr_Hf
296 2 HF1767   heatr_Hf_176     gaminr_Hf
297 2 HF1777   heatr_Hf_177     gaminr_Hf
298 2 HF1787   heatr_Hf_178     gaminr_Hf
299 2 HF1797   heatr_Hf_179     gaminr_Hf
300 2 HF1807   heatr_Hf_180     gaminr_Hf
```

```
301 2 TA1817   heatr_Ta_181     gaminr_Ta
302 2 TA1827   heatr_Ta_182     gaminr_Ta
303 2 W182_7   heatr_W_182      gaminr_W
304 2 W183_7   heatr_W_183      gaminr_W
305 2 W184_7   heatr_W_184      gaminr_W
306 2 W186_7   heatr_W_186      gaminr_W
307 2 RE1857   heatr_Re_185     gaminr_Re
308 2 RE1877   heatr_Re_187     gaminr_Re
309 2 IR1917   heatr_Ir_191     gaminr_Ir
310 2 IR1937   heatr_Ir_193     gaminr_Ir
311 2 AU1977   heatr_Au_197     gaminr_Au
312 2 HG1967   heatr_Hg_196     gaminr_Hg
313 2 HG1987   heatr_Hg_198     gaminr_Hg
314 2 HG1997   heatr_Hg_199     gaminr_Hg
315 2 HG2007   heatr_Hg_200     gaminr_Hg
316 2 HG2017   heatr_Hg_201     gaminr_Hg
317 2 HG2027   heatr_Hg_202     gaminr_Hg
318 2 HG2047   heatr_Hg_204     gaminr_Hg
319 2 PB2047   heatr_Pb_204     gaminr_Pb
320 2 PB2067   heatr_Pb_206     gaminr_Pb
321 2 PB2077   heatr_Pb_207     gaminr_Pb
322 2 PB2087   heatr_Pb_208     gaminr_Pb
323 2 BI2097   heatr_Bi_209     gaminr_Bi
324 2 RA2237   heatr_Ra_223     gaminr_Ra
325 2 RA2247   heatr_Ra_224     gaminr_Ra
326 2 RA2257   heatr_Ra_225     gaminr_Ra
327 2 RA2267   heatr_Ra_226     gaminr_Ra
328 3 AC2257   heatr_Ac_225     gaminr_Ac     dbeta_89225
329 3 AC2267   heatr_Ac_226     gaminr_Ac     dbeta_89226
330 3 AC2277   heatr_Ac_227     gaminr_Ac     dbeta_89227
331 3 TH2277   heatr_Th_227     gaminr_Th     dbeta_90227     dgamma_90227
332 3 TH2287   heatr_Th_228     gaminr_Th     dbeta_90228
333 3 TH2297   heatr_Th_229     gaminr_Th     dbeta_90229     dgamma_90229
334 3 TH2307   heatr_Th_230     gaminr_Th     dbeta_90230
335 3 TH2327   heatr_Th_232     gaminr_Th     dbeta_90232     dgamma_90232
336 3 TH2337   heatr_Th_233     gaminr_Th     dbeta_90233
337 3 TH2347   heatr_Th_234     gaminr_Th     dbeta_90234
338 4 PA2317   heatr_Pa_231     gaminr_Pa     dbeta_91231     dgamma_91231
339 3 PA2327   heatr_Pa_232     gaminr_Pa     dbeta_91232
340 3 PA2337   heatr_Pa_233     gaminr_Pa     dbeta_91233
341 4 U232_7   heatr_U_232      gaminr_U      dbeta_92232     dgamma_92232
342 4 U233_7   heatr_U_233      gaminr_U      dbeta_92233     dgamma_92233
343 4 U234_7   heatr_U_234      gaminr_U      dbeta_92234     dgamma_92234
344 4 U235_7   heatr_U_235      gaminr_U      dbeta_92235     dgamma_92235
345 4 U236_7   heatr_U_236      gaminr_U      dbeta_92236     dgamma_92236
346 4 U237_7   heatr_U_237      gaminr_U      dbeta_92237     dgamma_92237
347 4 U238_7   heatr_U_238      gaminr_U      dbeta_92238     dgamma_92238
348 3 U239_7   heatr_U_239      gaminr_U      dbeta_92239
349 3 U240_7   heatr_U_240      gaminr_U      dbeta_92240
350 3 U241_7   heatr_U_241      gaminr_U      dbeta_92241
351 3 NP2357   heatr_Np_235     gaminr_Np     dbeta_93235
352 3 NP2367   heatr_Np_236     gaminr_Np     dbeta_93236
353 4 NP2377   heatr_Np_237     gaminr_Np     dbeta_93237     dgamma_93237
354 4 NP2387   heatr_Np_238     gaminr_Np     dbeta_93238     dgamma_93238
355 3 NP2397   heatr_Np_239     gaminr_Np     dbeta_93239
356 3 PU2367   heatr_Pu_236     gaminr_Pu     dbeta_94236
357 3 PU2377   heatr_Pu_237     gaminr_Pu     dbeta_94237
358 4 PU2387   heatr_Pu_238     gaminr_Pu     dbeta_94238     dgamma_94238
359 4 PU2397   heatr_Pu_239     gaminr_Pu     dbeta_94239     dgamma_94239
360 4 PU2407   heatr_Pu_240     gaminr_Pu     dbeta_94240     dgamma_94240
361 4 PU2417   heatr_Pu_241     gaminr_Pu     dbeta_94241     dgamma_94241
```

```
362 4 PU2427   heatr_Pu_242     gaminr_Pu    dbeta_94242    dgamma_94242
363 3 PU2437   heatr_Pu_243     gaminr_Pu    dbeta_94243
364 3 PU2447   heatr_Pu_244     gaminr_Pu    dbeta_94244
365 3 PU2467   heatr_Pu_246     gaminr_Pu    dbeta_94246
366 4 AM2417   heatr_Am_241     gaminr_Am    dbeta_95241    dgamma_95241
367 4 AM2427   heatr_Am_242     gaminr_Am    dbeta_95242    dgamma_95242
368 4 AM42M7   heatr_Am_242m1   gaminr_Am    dbeta_95342    dgamma_95342
369 4 AM2437   heatr_Am_243     gaminr_Am    dbeta_95243    dgamma_95243
370 3 AM2447   heatr_Am_244     gaminr_Am    dbeta_95244
371 3 AM44M7   heatr_Am_244m1   gaminr_Am    dbeta_95344
372 3 CM2417   heatr_Cm_241     gaminr_Cm    dbeta_96241
373 4 CM2427   heatr_Cm_242     gaminr_Cm    dbeta_96242    dgamma_96242
374 4 CM2437   heatr_Cm_243     gaminr_Cm    dbeta_96243    dgamma_96243
375 4 CM2447   heatr_Cm_244     gaminr_Cm    dbeta_96244    dgamma_96244
376 4 CM2457   heatr_Cm_245     gaminr_Cm    dbeta_96245    dgamma_96245
377 4 CM2467   heatr_Cm_246     gaminr_Cm    dbeta_96246    dgamma_96246
378 3 CM2477   heatr_Cm_247     gaminr_Cm    dbeta_96247
379 4 CM2487   heatr_Cm_248     gaminr_Cm    dbeta_96248    dgamma_96248
380 3 CM2497   heatr_Cm_249     gaminr_Cm    dbeta_96249
381 3 CM2507   heatr_Cm_250     gaminr_Cm    dbeta_96250
382 3 BK2497   heatr_Bk_249     gaminr_Bk    dbeta_97249
383 3 BK2507   heatr_Bk_250     gaminr_Bk    dbeta_97250
384 4 CF2497   heatr_Cf_249     gaminr_Cf    dbeta_98249    dgamma_98249
385 4 CF2507   heatr_Cf_250     gaminr_Cf    dbeta_98250    dgamma_98251
386 3 CF2517   heatr_Cf_251     gaminr_Cf    dbeta_98251
387 3 CF2527   heatr_Cf_252     gaminr_Cf    dbeta_98252
388 3 CF2537   heatr_Cf_253     gaminr_Cf    dbeta_98253
389 3 CF2547   heatr_Cf_254     gaminr_Cf    dbeta_98254
390 2 ES2537   heatr_Es_253     gaminr_Es
391 4 ES2547   heatr_Es_254     gaminr_Es    dbeta_99254    dgamma_99254
392 2 ES2557   heatr_Es_255     gaminr_Es
393 3 FM2557   heatr_Fm_255     gaminr_Fm    dbeta_100255
```

Nuclear and Science Engineering Division
Argonne National Laboratory
9700 South Cass Avenue, Bldg. 208
Argonne, IL 60439-4842

www.anl.gov